Transient Complex Formation in CO_2−Hexafluorobenzene Mixtures: a Combined Raman and ab Initio Investigation

M. Besnard,*,† M. Isabel Cabaço,‡ and Y. Danten†

Institut des Sciences Moléculaires, CNRS (UMR 5255), Université Bordeaux 1, 351 Cours de la Libération 33405 Talence Cedex, France, Centro de Física Atómica, Universidade de Lisboa, Avenida Prof. Gama Pinto 2, 1694-003 Lisboa Codex, Portugal, and Departamento de Física, Instituto Superior Técnico, Universidade Técnica de Lisboa, Avenida Rovisco Pais 1049-001 Lisboa, Portugal

Received: July 31, 2008; Revised Manuscript Received: October 27, 2008

The polarized and depolarized Raman spectra of CO_2 in binary mixtures with hexafluorobenzene have been measured in the dense phase along the isotherm 313 K as a function of concentration (0.03−0.7 molar fraction in CO_2) by varying the pressure (0.5−6.2 MPa). Experimental observations in the ν_2 bending region, in the $\nu_1-2\nu_2$ Fermi resonance dyad, and in the spectral domain between the Fermi dyad peaks on CO_2 are reported. These results are discussed in comparison with those obtained in previous studies on $CO_2-C_6H_6$ and CO_2−acetone mixtures. We conclude in agreement with previous investigations that CO_2 molecules can probe two environments. In one of them carbon dioxide interacts "specifically" with hexafluorobenzene molecules to form a transient heterodimer, whereas in the other environment CO_2 interacts "nonspecifically" with its neighbors. New ab initio calculations reported here allow rationalizing most of the experimental results. However, the observation of weak spectral features (bending mode and Fermi dyad regions) shows that a slight departure from the predicted structure (C_{6v} symmetry) should exist in the dense phase. Finally, the greater solubility of CO_2 in perfluorinated benzene versus perhydrogenated benzene has been discussed on the basis of this study in connection with thermodynamic measurements interpreted in the scaled particle theory framework.

1. Introduction

In a recent series of investigations, we have shown that transient heterodimers formed by CO_2 with an organic molecule can be detected using Raman spectroscopy in binary mixtures obtained by introducing under pressure supercritical carbon dioxide in an organic liquid solvent.[1−3] We have also shown that ab initio calculations although treating "idealized" systems characterized by a few interacting molecules in the absence of a thermal bath constitute a valuable guideline in the analysis of spectroscopic results obtained for dense phase systems. This conclusion has been reached by recognizing that the elementary act of transient complex formation considered in the calculation matches closely the spatial and temporal spectroscopic observation conditions.

It is in the context of these systematic investigations that we have studied the system $CO_2-C_6H_6$ and decided to undertake this new investigation of the $CO_2-C_6F_6$ binary mixtures. Several reasons have motivated the choice of this fluorinated benzenic molecule. First of all, we already do know that benzene and perfluorinated benzene although having similar molecular shapes and absolute magnitudes of their quadrupole moments have quite different short-range structural ordering in the liquid phase.[4−6] In addition, if charge transfer interactions are pertinent in CO_2 mixtures, we expect on simple grounds that heterodimer formation will lead to rather different geometries of the complexes. Indeed, in $CO_2-C_6H_6$ the interactions take place mostly between the carbon atom of CO_2 (playing the role of Lewis acid center) and the π electron cloud of the benzene ring acting as the basic center.[3,7] This leads to a complex having a plateaulike structure with the CO_2 molecular axis rather parallel to the benzene plane. In contrast, for the perfluorinated molecule, the electronic depletion due to the electronegative fluorine atoms is located within the carbon ring center, making it a Lewis acid center. Therefore, the structure in which the lone pair of the oxygen of CO_2 interacts with the core of the ring is expected for the complex. It is on the basis of intermolecular interactions that the higher solubility of fluorinated (versus hydrogenated) materials would be understood. For instance, it has been argued that the higher solubility of fluorinated polymers dissolved in supercritical (SC) CO_2 might result from the interaction of CO_2 with the dipoles of C−F bonds as shown by IR spectroscopic studies of the bending mode of CO_2.[8,9]

However, as far as we know, ab initio calculations and vibrational spectra for this system have not been reported and for this reason will be presented and discussed in the current paper to rationalize the experimental data. Clearly, this new investigation discussed in comparison with the previous one on $CO_2-C_6H_6$ should bring insight into the CO_2 heterodimer formation in mixtures in which the intermolecular interactions are expected to be different.

The other motivation to undertake the current study is connected with the field of SC fluids. It has been argued that perfluorinated SC fluids have a greater solvating power compared to those involving the corresponding perhydrogenated molecules.[10,11] However, the molecular interpretation of this situation is still a matter of debate as experimental or theoretical investigations in the literature bring contradictory evidence concerning the origin of the existence of particular interactions which are at the basis of the solubility enhancement in

* Corresponding author. Telephone: +33 5 40006357. Fax: +33 5 4000 8402. E-mail: m.besnard@ism.u-bordeaux1.fr.
† Université Bordeaux 1.
‡ Universidade de Lisboa and Universidade Técnica de Lisboa.

10.1021/jp8068267 CCC: $40.75
Published on Web 12/10/2008

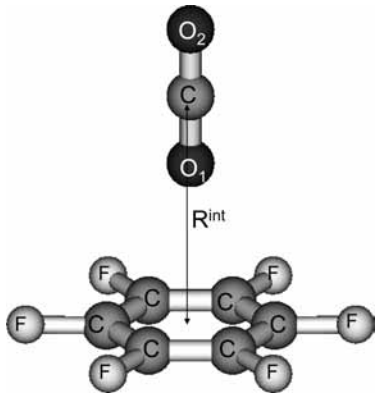

Figure 1. Equilibrium structure of the $CO_2-C_6F_6$ complex calculated at the MP2/aug-cc-pV(D,T)Z computational level.

fluorinated compounds.[12] Clearly, these debates point out the need to have a better understanding at a microscopic level of the nature and time scale of the intermolecular interactions in fluorinated solvent compared with their homologous perhydrogenated ones.[13]

The aim of this paper is to address the question of the heterodimer formation in CO_2−perfluorinated benzene mixtures as seen by Raman scattering in the spectral domains that we have shown in our previous studies to be adapted to the detection of the spectral signatures of transient species. The paper will be organized as follows. First of all, we will present ab initio calculations performed on this system to provide the structural and vibrational properties of the heterodimer. Then, we will present the experimental observations using Raman spectroscopy on CO_2 in the forbidden ν_2 bending region, in the $\nu_1-2\nu_2$ Fermi resonance dyad, and in the spectral domain between the Fermi dyad peaks. In the last part of the paper, we will discuss the reported experimental observations in light of the ab initio modeling to provide a picture of the intermolecular interactions in the $CO_2-C_6F_6$ mixture. Finally, we will comment on the connection between the local ordering and the solubility analyzed using the scaled particle theory (SPT).[14,15]

2. Structural and Vibrational Properties of the Dimer $CO_2-C_6F_6$

2.1. Details of the Calculations. Ab initio calculations of the isolated $CO_2-C_6F_6$ complex have been carried out using the Gaussian 03 suite.[16] For such a van der Waals complex the stabilization process mainly relies on the electron exchange correlation. For this reason, the optimized geometry has been achieved at the second-order Møller−Plesset (MP2) level of perturbation theory[17] using the correlation-consistent polarized valence double zeta (cc-pVDZ) and triple zeta (cc-pVTZ) basis sets, respectively[18−20] augmented by diffuse functions (labeled using the prefix "aug-").[21] No symmetrical considerations have been held initially during the geometry optimization procedure, even if the global energy minimum structure has been finally found having an axial C_{6v} symmetry. The calculated interaction energy was corrected from the basis set superposition error (BSSE) using the counterpoise (CP) technique.[22]

2.2. Structure and Binding Energy. The fully optimized structure of the $CO_2-C_6F_6$ complex is schematically displayed in Figure 1, and the main calculated geometric parameters have been reported in Table 1. In this structure (having C_{6v} symmetry), the CO_2 molecule is along the C_6 symmetry axis with an O-atom pointing toward the center of the aromatic ring minimizing the overlap between the orbitals of both partners.

TABLE 1: Calculated Equilibrium Structure of the Dimer $C_6F_6 \cdot CO_2$ (C_{6v} Symmetry) at the MP2 level of Perturbation Using Augmented Correlation-Consistent Polarized Valence Double/Triple Zeta Basis Sets[18−21]

basis set	aug-cc-pVTZ	aug-cc-pVDZ
electron energy (H)	−1014.845 429 152 5	−1014.015 962 233 3
parameters		
$R^{(int)}$ (Å)	4.111	4.030
d_{CC} (Å)	1.389	1.400
d_{CF} (Å)	1.330	1.347
d_{O_1C} (Å)	1.172	1.182
d_{O_2C} (Å)	1.169	1.179
binding energy (kcal/mol)		
$\Delta E_{int}^{(cor)}$	−2.19	−1.88
$\Delta E_{int}^{(BSSE)}$	+1.06	+2.22
$\Delta E_{int}^{(MP2)}$	−3.10	−3.36
$\Delta E_{int}^{(ZPE)}$	n.c.	+0.56

This equilibrium structure is mainly stabilized through an electron donor−acceptor (EDA) interaction mechanism. The CP-corrected interaction energies are evaluated at about −1.9 (VDZ) and −2.2 kcal/mol (VTZ), respectively. Although the electron correlation (dispersion) energy still represents the main contribution to the stabilization of this complex (cf. $\Delta E_{int}^{(MP2)}$ values in Table 1), we notice that this contribution is less than that found for the $CO_2-C_6H_6$ complex.[3] Thus, in their equilibrium structures, the $CO_2-C_6F_6$ complex is found slightly less stable than $CO_2-C_6H_6$ (0.5 kcal/mol). Other local minimum energy structures have been searched by exploring the calculated interaction energy surface (IPS) for different relative orientational configurations of the $CO_2-C_6F_6$ dimer. At the MP2/aug-cc-pV(D,T)Z computation level, these local energy minimum structures do not correspond with stationary points and will not be further discussed here because they are without real incidences for the purpose of the present study. Incidentally, we notice that, among these local energy minimum structures, the C_{2v} symmetry structure in which CO_2 is parallel to the aromatic plane has been found as a transition state with a BSSE-corrected interaction energy of about −1.7 kcal/mol.

2.3. Vibrational Analysis. The vibrational analysis of the $C_6F_6-CO_2$ complex has been carried out within the standard Wilson FG matrix formalism[23] implemented in the Gaussian 03 suite[16] from the equilibrium structure predicted at the MP2/aug-cc-pVDZ computational level. The highest quality aug-cc-pVTZ basis set precluded us from carrying out the vibrational analysis of this complex at the MP2 level of the perturbation theory. However, previous investigations showed that the calculated IR and Raman intensities (as well as the frequency transitions) using the VTZ basis set lead qualitatively to similar spectral signatures with only comparatively small deviations from values calculated at the MP2/aug-cc-pVDZ level.[24] The computed harmonic frequencies, IR intensities, and Raman activities (and depolarization ratio) associated with the internal modes of the $C_6F_6-CO_2$ complex have been reported in Table 2 and compared with those of the isolated moieties. The vibrational anharmonicity effects can be taken into account using a frequency scaling factor of 0.960.[25] Clearly, vibrational modes particularly sensitive to $CO_2-C_6F_6$ complex formation in the axial conformation are not apparent. Due to the symmetry of the complex (C_{6v} symmetry), the ν_2 bending mode of CO_2 remains doubly degenerate and there is no frequency splitting under the complex formation. However, the IR absorption intensity of this mode decreases significantly by about 60% whereas the Raman line remains inactive. The frequency

TABLE 2: Calculated Frequency Transitions, IR Intensities, and Raman Intensities of the Dimer $C_6F_6 \cdot CO_2$ (C_{6v} Symmetry) at the MP2/aug-cc-pVDZ level (Left) and Comparison with the Corresponding Spectral Properties of Isolated Moieties (Right)[a]

MP2/aug-cc-pVDZ level					Isolated Moieties			
sym	ν_{cal} (cm^{-1})	I_{IR} (km/mol)	I_{Raman} (Å^4/amu)	CO_2 modes	sym	ν_{cal} (cm^{-1})	I_{IR} (km/mol)	I_{Raman} (Å^4/amu)
E_1	653.5	17.3	~0	ν_2(OCO)	Π_u	655.5	43.0	inactive
A_1	1305.4	0.1	42.1 (0.26)	ν_1(CO)	Σ_g	1305.4	inactive	33.4 (0.14)
A_1	2414.7	575.6	0.23 (0.67)	ν_3(CO)	Σ_u	2379.2	567.6	inactive
MP2/aug-cc-pVDZ level					Isolated Moieties			
sym	ν_{cal} (cm^{-1})	I_{IR} (km/mol)	I_{Raman} (Å^4/amu)	C_6F_6 modes	sym	ν_{cal} (cm^{-1})	I_{IR} (km/mol)	I_{Raman} (Å^4/amu)
A_1	216.8	5.4	0.15 (0.41)	$\nu_4(\gamma_{CF})$	A_{2u}	210.6	4.9	inactive
E_2	264.3	inactive	0.215 (0.75)	$\nu_{17}(\beta_{CF})$	E_{2g}	264.4	inactive	0.1 (0.75)
E_1	311.9	1.4	inactive	$\nu_{14}(\beta_{CF})$	E_{1u}	312.4	1.5	inactive
E_1	372.1	~0	3.0 (0.75)	$\nu_{11}(\gamma_{CF})$	E_{1g}	361.2	inactive	2.9 (0.75)
E_2	438.4	inactive	4.9 (0.75)	$\nu_{18}(\beta_{CCC})$	E_{2g}	436.0	inactive	4.5 (0.75)
A_1	553.2	~0	22.3 (0.11)	ν_2(CC)	A_g	553.4	inactive	30.0 (0.06)
E_1	996.3	240.9	~0	ν_{13}(CC)	E_{1u}	997.2	247.0	inactive
E_2	1146.4	inactive	0.6 (0.75)	ν_{16}(CC)	E_{2g}	1145.5	inactive	1.4 (0.75)
A_1	1511.0	1.7	3.5 ($<2 \times 10^{-3}$)	ν_1(CF)	A_{1g}	1511.6	inactive	3.5 ($<2 \times 10^{-3}$)
E_1	1551.3	320.2	~0	ν_{12}(CF).	E_{1u}	1549.6	327.6	inactive
E_2	1701.2	inactive	6.9 (0.75)	ν_{15}(CF)	E_{2g}	1688.3	inactive	4.4 (0.75)

[a] The depolarization ratio values are given in parentheses.

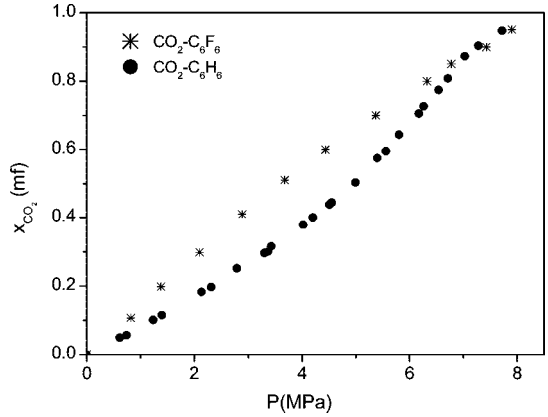

Figure 2. Solubility of CO_2 in hexafluorobenzene compared with that of CO_2 in benzene at 313 K as a function of pressure.

transition of the ν_1 symmetric CO stretching mode is nearly unchanged under the complex formation (even if a weak induced IR absorption can be expected, cf. Table 2) while the corresponding intense polarized Raman line is slightly enhanced by 20% compared with isolated CO_2. In contrast, the intense IR line of the ν_3 antisymmetric mode of CO_2 is found significantly shifted toward higher frequencies (35.5 cm^{-1}) by interactions with the aromatic ring, although its intensity is nearly unchanged. However, a weak induced Raman activity can be also expected in the axial configuration of the $C_6F_6-CO_2$ complex.

3. Experimental Section

3.1. Experimental Conditions. The comparison of the values of the molar fraction of CO_2 diluted in the dense phase of the benzene$-CO_2$ and hexafluorobenzene$-CO_2$ binary mixtures interpolated from published values[10,26] as a function of the pressure at the same temperature is presented in Figure 2.

It appears that the solubility in hexafluorobenzene is always greater than that in benzene with a maximum for their difference close to 4 MPa. For that pressure, the solubility of CO_2 in C_6F_6 is about 50% greater than in benzene. This result supports the statement referred to in the Introduction concerning the greater solvating power of fluorinated compounds compared to their perhydrogenated homologues. We should remark that the pertinent variable for discussing the evolution of the solubility should be the density instead of the pressure.[27] However, the evolution of the density with the composition of the dense phase of the binary mixture has not been reported. Nevertheless, we can estimate the density variation as follows. At very low molar fraction of CO_2 in C_6F_6 (very low CO_2 pressures) the density of the mixture is close to that of C_6F_6, i.e., about 1.57 g cm^{-3} (at 313 K).[4] A glance at Figure 2 shows that, for pressures greater than 7 MPa, the molar fraction x_{CO_2} is close to 0.9 in either the benzene or the hexafluorobenzene mixtures. In such highly concentrated mixtures in CO_2, because the amount of benzenic material is rather small, we can assume that the densities of the solutions are very close. At these CO_2 molar fractions, the values of the density of the CO_2-benzene mixture reported in the literature differ by at most 20% from the density of pure benzene, i.e., are within the range 0.7$-$0.87 g cm^{-3}.[28]

The Raman spectra were measured on a Jobin-Yvon HR8000 spectrometer with a Spectra Physics krypton ion laser source operating at a wavelength of 752.5 nm with a power of 150 mW. The polarized I_{VV} and depolarized I_{HV} spectra were recorded using backscattering geometry. Two spectral ranges, from 315 to 1140 cm^{-1} and from 1200 to 1450 cm^{-1} have been recorded with a resolution of 1.8 cm^{-1} using a 600 lines mm^{-1} grating. The latter spectral domain has been also analyzed with a resolution of 0.5 cm^{-1} using an 1800 lines mm^{-1} grating. To improve the signal-to-noise ratio, several spectra have been accumulated for typical times of 16 and 4 min, respectively, in the referred spectral ranges. In order to take accurate line positions, the spectrometers have been calibrated by recording different emission lines of a neon bulb. We have used the pressure bench and the Raman cell equipped with fused silica windows previously described[29] to work in the 0.1$-$10 MPa pressure range at $T = 313$ K. For the measurements in the mixtures, we initially filled the cell with C_6F_6 (Aldrich, 99% purity) in order to ensure that after addition of CO_2 (Air Liquide, purity 99.995%) and pressurization the incident laser beam always impinges on the liquid phase. The mixtures were continuously stirred using a magnet activated by a rotating magnetic field. All the spectra have been recorded after an equilibration time greater than 2 h.

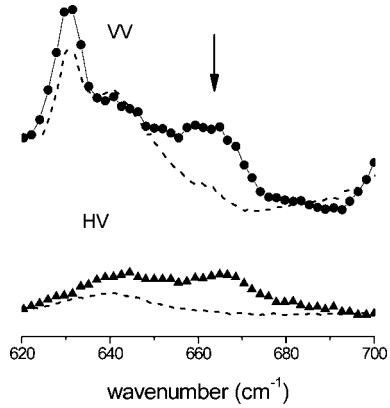

Figure 3. Polarized I_{VV} (−●−●−) and depolarized I_{HV} (−▲−▲−) Raman spectra of the ν_2 bending vibrational mode (arrow) of CO_2 at 313 K in CO_2−hexafluorobenzene mixture ($x_{CO_2} = 0.71$). The polarized and depolarized spectra of pure hexafluorobenzene (---) at 313 K are also presented for comparison.

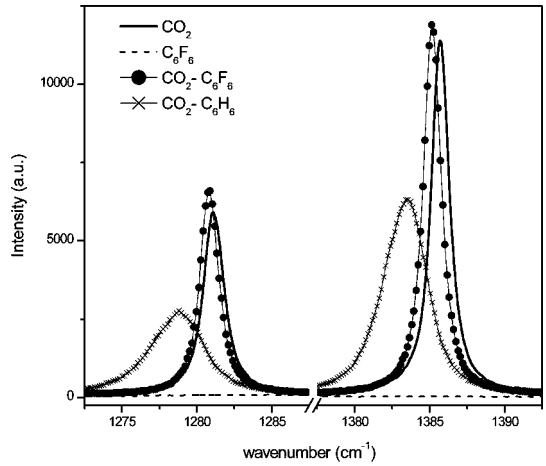

Figure 4. Comparison of the polarized Raman spectra of the CO_2 Fermi dyad at 313 K in CO_2−hexafluorobenzene mixture ($x_{CO_2} = 0.71$), in CO_2−benzene mixture ($x_{CO_2} = 0.68$), and in pure CO_2 (19 MPa, ρ = 830 kg m^{-3}). The polarized spectrum of pure hexafluorobenzene is also presented.

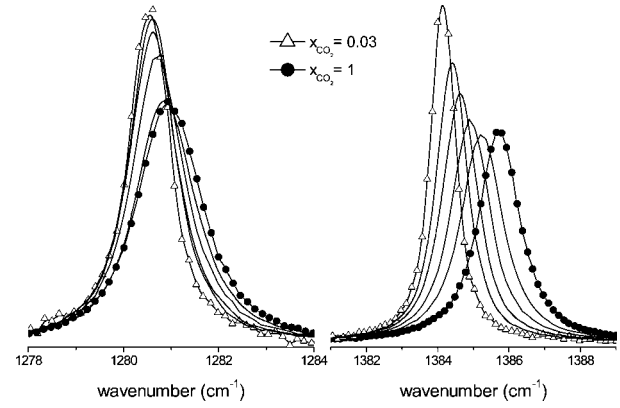

Figure 5. Evolution of polarized Raman spectra of the CO_2 Fermi dyad at increasing CO_2 molar fraction in the binary mixtures at 313 K. The intensities have been normalized to the total integrated intensity of each component of the dyad. The spectra are displayed for the molar fractions 0.03, 0.16, 0.30, 0.48, 0.71, and 1 from left to right on each dyad component (pure CO_2 at 19 MPa).

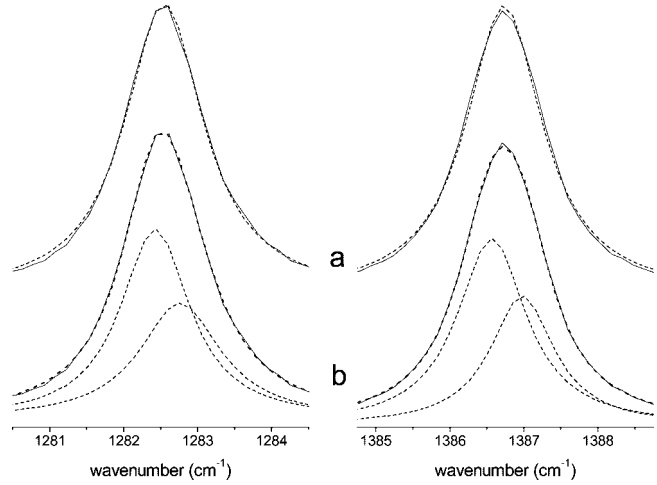

Figure 6. Experimental and calculated polarized Raman spectra in the CO_2 Fermi dyad domain of CO_2−hexafluorobenzene mixture ($x_{CO_2} = 0.50$) at 313 K. The calculated band shapes have been obtained by fitting (a) one Lorentzian profile and (b) two Lorentzian profiles.

3.2. Experimental Results. ***3.2.1. The ν_2 Bending Mode Spectral Domain.*** The polarized I_{VV} and depolarized I_{HV} Raman spectra of neat liquid perfluorinated benzene, measured under its vapor pressure at 313 K, are displayed in the spectral range 600−700 cm^{-1} in Figure 3. Upon addition of CO_2 at pressures greater than 5 MPa, a new weak, slightly polarized band is detected in the spectrum as seen from the comparison with that of pure hexafluorobenzene (Figure 3). The band center positions of the I_{VV} and I_{HV} profiles are found at about 664 cm^{-1}.

3.2.2. Polarized Fermi Dyad Spectral Domain. The polarized Raman spectrum of CO_2 diluted in C_6F_6 ($x_{CO_2} = 0.71$) is compared in the Fermi domain with that measured for neat CO_2 at about the same density in Figure 4. In this spectral domain, the pure hexafluorobenzene spectrum reduces to an almost flat background and does not contribute to the spectra of the mixture (Figure 4). The CO_2 spectrum in the mixture exhibits two intense peaks as those observed for neat CO_2. The band center positions of the Fermi doublet are slightly shifted toward lower frequency, and the widths of each of the two components increase slightly with the CO_2 concentration in the mixture. The small perturbations of the spectra of CO_2 diluted in C_6F_6 should be contrasted with the marked perturbations (both significant red shift and broadening of the dyad peaks) observed on the spectra of carbon dioxide diluted in benzene (Figure 4). The polarized Raman spectra of the CO_2 Fermi dyad measured in the binary mixtures at increasing carbon dioxide molar fraction are displayed in Figure 5. The intensities have been normalized to the total integrated intensity of each component of the dyad. It is apparent that spectral perturbations still remain modest as the CO_2 concentration increases in the mixture.

We have then proceeded to a band shape analysis. We note that, for pure carbon dioxide or for this molecule diluted in a binary mixture, the analysis of the dyad band shape requires a fit of two Lorentzian profiles on each doublet component in order to have very good fits.[1,3,30] We indeed checked that for the present system good spectral fits are only achieved with the same type of analysis (Figure 6).

The evolution with the CO_2 concentration of the obtained results is presented in Figures 7 and 8 using the previous convention labeling the two components in the high (respectively low) frequency peak of the Fermi doublet as U_1 and U_2 (respectively L_1 and L_2). The label 1 (respectively 2) characterizes the fitted profile centered at the lowest frequency (respectively higher) in each peak of the Fermi dyad.

We found that the band center frequencies values of the four fitted Lorentzians increase almost linearly with x_{CO_2} (Figure 7). The extrapolated values of the band center of the L_2 and U_2

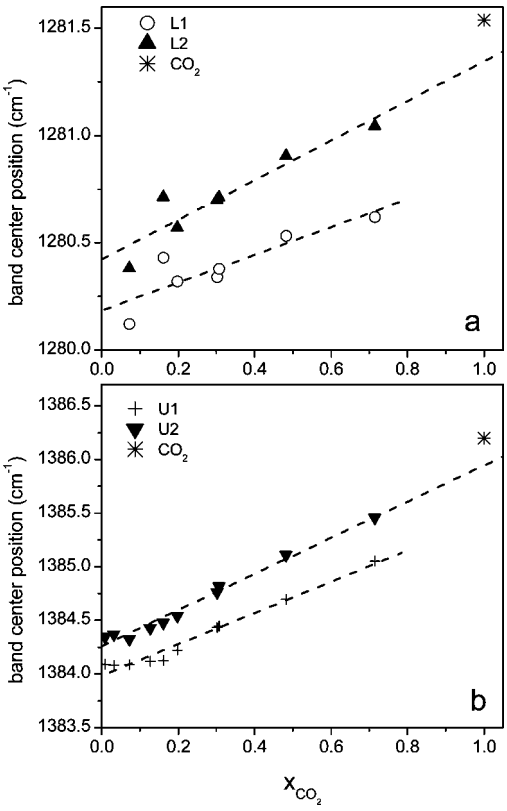

Figure 7. Evolution with the CO_2 concentration of the band center position of the Lorentzian profiles fitted to the polarized Raman spectra of the CO_2 in the Fermi dyad domain of CO_2−hexafluorobenzene mixtures at 313 K: (a) (○) L_1, (▲) L_2; (b) (+) U_1, (▼) U_2. The values for pure CO_2 (19 MPa, $\rho = 830$ kg m^{-3}) are displayed for comparison (∗).

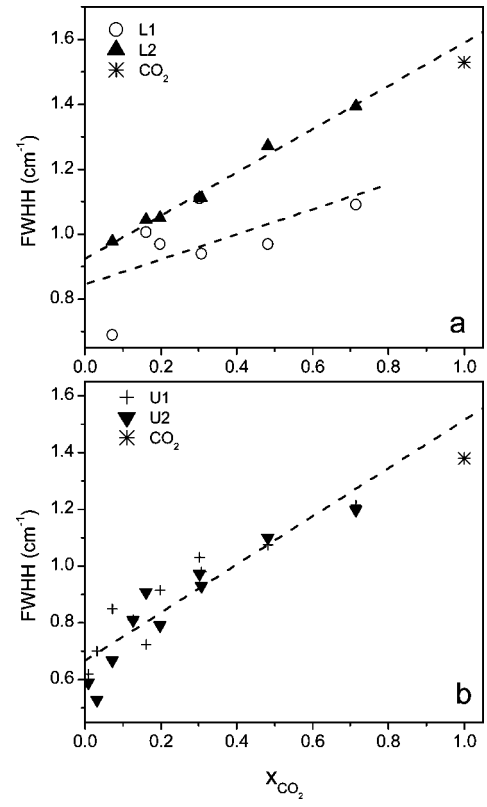

Figure 8. Evolution with the CO_2 concentration of the full width at half-height (FWHH) of the fitted Lorentzian profiles to the polarized Raman spectra in the CO_2 Fermi dyad domain of CO_2−hexafluorobenzene mixtures at 313 K: (a) (○) L_1, (▲) L_2; (b) (+) U_1, (▼) U_2. The values for pure CO_2 (19 MPa, $\rho = 830$ kg m^{-3}) are displayed for comparison (∗).

profiles agree with the corresponding ones for CO_2 at equivalent density (see section 3.1).

The values of the widths L_1, L_2 and U_1, U_2 of the profiles increase linearly with the CO_2 concentration. We notice that the values of the widths of the upper components are almost the same (Figure 8b). The extrapolated value of the width of L_2 agrees again with the corresponding value for CO_2 at equivalent density.

The ratio $R = I_U/I_L$, where I denotes the integrated intensity of the upper (U) and lower (L) components of the Fermi dyad, is almost constant within experimental uncertainties with a value of about 1.75 (Figure 9a), and the extrapolated value agrees with that of pure CO_2. We have also reported (Figure 9b) the ratios $R_L = I_{L_2}/(I_{L_1} + I_{L_2})$ and $R_U = I_{U_2}/(I_{U_1} + I_{U_2})$, where I denotes the integrated intensity of each of the four components fitted in the polarized Fermi dyad profiles. These ratios represent the relative weight of the integrated intensity of the higher frequency peak fitted on each component of the dyad. We found that the values of these ratios, although exhibiting some scatter, have a mean value of 0.5 ± 0.1.

3.2.3. Spectral Domain between the Dyad Peaks. In the spectra of the mixture, the presence of a very weak and broad feature (absent in pure C_6F_6) centered at about 1330 cm^{-1} is detected. This band is polarized, as seen from the comparison of the polarized and depolarized spectra (Figure 10).

4. Interpretation

The ensemble of experimental results reported here can be rationalized in light of the conclusions that we have obtained in the studies of CO_2 in binary mixtures (CO_2 in acetone and in benzene), in which we have shown that the molecules exist in two different environments.[1,3] According to these investigations, we may infer that, in the current study, the formation of a transient complex is provided by four different spectral signatures. Two of them are associated with the features observed in the ν_2 domain and in the spectral region between the Fermi dyad peaks.

The existence of a second environment is suggested by the need to use two different profiles to describe each of the components of the dyad. The first one is associated with CO_2 molecules "specifically" interacting with hexafluorobenzene molecules and engaged in the formation of a heterodimer. The second one corresponds to carbon dioxide mostly interacting with other CO_2 molecules (in mixtures in which C_6F_6 is highly diluted) or in a "nonspecific" manner with C_6F_6 molecules (in concentrated C_6F_6 mixture). We referred to this latter situation as the "free" CO_2 environment, although the molecules interact with their neighbors.

In agreement with our previous study, we can associate the component of higher frequency (U_2 and L_2) in each peak of the Fermi dyad with the "free" molecules as seen from Figures 7−9 because the extrapolated values of the spectral parameters agree with the corresponding values for pure CO_2 at equivalent density. Assuming that Raman polarized cross sections are unaffected by molecular aggregation,[1] we conclude from the values of the ratios R_U and R_L that that the proportion of CO_2 engaged in the heterodimers is about 50% of the total CO_2 concentration.

Direct evidence about the formation of a complex can be also obtained from the study of the band shape of the depolarized

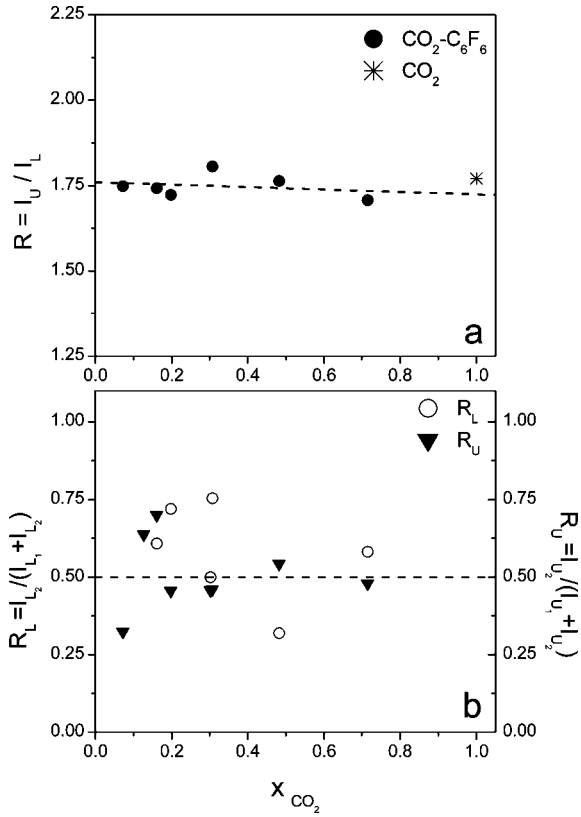

Figure 9. Evolution with the CO_2 concentration of the ratio of the integrated intensities of the polarized profiles fitted in the Fermi dyad of CO_2 in the mixtures at 313 K. (a) $R = (I_{U_1} + I_{U_2})/(I_{L_1} + I_{L_2})$. The corresponding R value for pure CO_2 (19 MPa, ρ = 830 kg m^{-3}) is displayed for comparison (∗). (b) (○) $R_L = I_{L_2}/(I_{L_1} + I_{L_2})$ and (▼) $R_U = I_{U_2}/(I_{U_1} + I_{U_2})$.

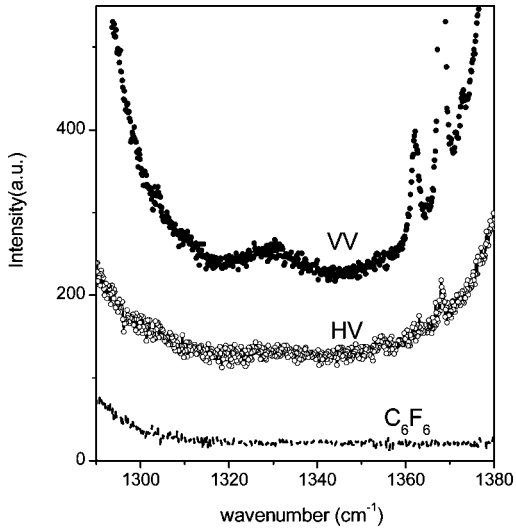

Figure 10. Polarized I_{VV} and depolarized I_{HV} Raman spectra in the spectral domain between the CO_2 Fermi dyad peaks in the CO_2−hexafluorobenzene mixture at 313 K (—), x_{CO_2} = 0.71. The polarized spectrum of hexafluorobenzene is given for comparison.

profiles. Recall that depolarized band shapes are governed by both vibrational and rotational relaxation processes in contrast to polarized profiles which are only influenced by the vibrational process. Our previous study of the CO_2−benzene mixture showed that the rotational dynamics of CO_2 involved in the formation of the complex is hindered.[3] We have reported in Figure 11a the depolarized profile associated with the Fermi dyad of pure CO_2. Each peak exhibits a narrow central Q branch

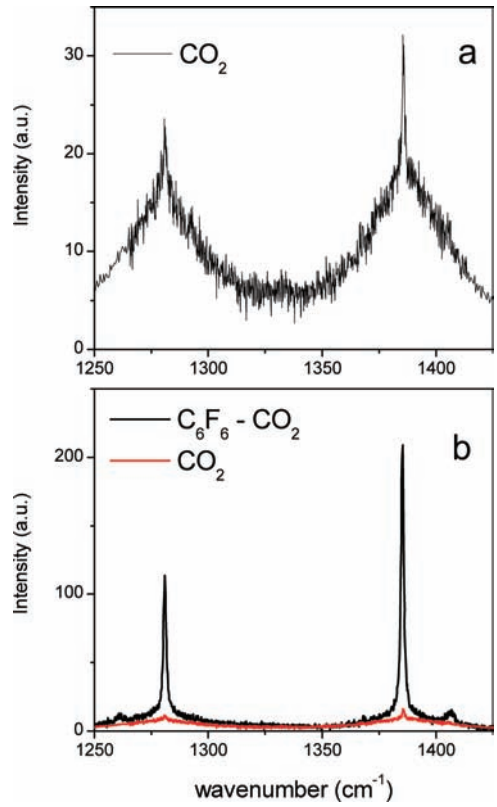

Figure 11. Depolarized Raman spectra in the Fermi dyad region at 313 K: (a) pure CO_2; (b) comparison of the spectra of CO_2 diluted in hexafluorobenzene (x_{CO_2} = 0.71) with that of pure CO_2 (ρ = 830 kg m^{-3}) after applying the normalization process described in the text (section 4).

superimposed on a very broad profile which is the signature of the rotational contribution of CO_2.[31] The broad feature shows that the rotation of the molecule, although perturbed by interaction with its neighbors in the dense fluid, is only slightly hindered and that the rotational dynamic is quite fast (subpicosecond regime), as has been reported.[32,33]

Considering now the mixture, we expect that the depolarized profile associated with CO_2 in its "free" environment can be approximated by the profile of pure CO_2 at equivalent density (Figure 11a). Therefore, we have compared the CO_2 and $CO_2-C_6F_6$ spectra. In order to simulate the relative contribution of the spectrum of "free" CO_2 in the spectra of the mixture, we have proceeded as follows. We have first normalized the spectra of pure CO_2 and of the $CO_2-C_6F_6$ mixture to the same integrated intensity. Assuming that the Raman depolarized cross sections are unaffected by molecular aggregation and because the estimated contribution of the "free" CO_2 is given by $R_U = R_L$ = 0.5 (cf. section 3.2.2), we have multiplied the intensity of the pure CO_2 spectrum by this factor (Figure 11b). It appears that the intensity of the spectrum of carbon dioxide in the mixture is concentrated in a narrow spectral domain close to the Q branch of the pure CO_2 spectrum. However, we note that the value of its intensity is much greater than that of the pure CO_2 Q branch. We also see that the shape of the wings of the CO_2 profile in the mixture corresponds fairly well to the broad component of the spectrum of pure CO_2 (Figure 11b). Therefore, the spectrum of $CO_2-C_6F_6$ can be considered as made of two contributions. The broad contribution corresponds to the "free" CO_2, whereas the narrow, intense band observed in the "free" CO_2 Q branch is assigned to CO_2 specifically interacting with C_6F_6. We also conclude that the rotational dynamics of CO_2 is

greatly different in the two environments. In the free environment the reorientational motion of CO_2 remains as fast as in pure CO_2 at an equivalent density as indicated by the presence of a Q branch accompanied by a broad component. In contrast, the rotational dynamics of carbon dioxide in the second environment is comparatively strongly hindered as shown by the fact that only a single intense narrow (Lorentzian) line is observed. Indeed, as a consequence of the rotational hindering, the Q branch and the broad component observed on the spectrum of a free rotor merge and collapse to lead to a single narrow line. Therefore the rotational hindering observed is consistent with the transient complex formation proposed here. Clearly, we can infer that the signature of the two types of environments detected on the polarized profiles is confirmed by the analysis of the depolarized profiles.

The order of magnitude of the orientational correlation time τ_{2R} characterizing the tumbling motion of the main symmetry axis of the CO_2 molecule can be obtained from the widths $\Delta\nu$ of the isotropic (almost I_{VV} here) and anisotropic (I_{HV}) Lorentzian profiles fitted on the Fermi dyad according to[34]

$$\tau_{2R} = [\pi c(\Delta\nu_{aniso} - \Delta\nu_{iso})]^{-1} \quad (1)$$

This formula has been applied to the isotropic and anisotropic profiles associated with L_1 and U_1 and led to a common value of 35 ps for the correlation time τ_{2R}. This value is much greater than that of the correlation time of pure CO_2[32] (about 0.3 ps) and confirms our conclusions about the strong hindering of the tumbling motion of CO_2 interacting with hexafluorobenzene.

It is interesting to note that although the approach used here concerning the treatment of the rotational motion has not been developed for band shapes in resonance, it led to a consistent value for the correlation time extracted from the lower and upper components of the dyad as we pointed out in the $CO_2-C_6H_6$ mixtures.

5. Discussion

All the experimental findings reported here can be interpreted in terms of a transient $CO_2-C_6F_6$ complex formation as found for the CO_2−benzene mixture. However, we notice that the perturbations of the spectra of CO_2 diluted in C_6F_6 are quite different from those observed in benzene. The bending mode of carbon dioxide is hardly detected in C_6F_6 mixtures, whereas it is easily observed in benzene. The Fermi dyad of CO_2 in $CO_2-C_6F_6$ is weakly perturbed in comparison with that in $CO_2-C_6H_6$ (see Figure 4 and section 3). For instance, the red shift of the band center position of the dyad peaks varies from about 7 to 3 cm^{-1} with concentration (x_{CO_2} ranging from 0.1 to 0.7) in C_6H_6 mixtures, whereas this variation is from 1.25 to 0.75 cm^{-1} in C_6F_6 mixtures. The values of the widths of the dyad peaks in benzene are about 3 times greater than those observed in C_6F_6. Moreover, the ratio R decreases with the CO_2 concentration in the benzene mixture, whereas it is almost constant in the hexafluorobenzene mixture (Figure 9).

Ab initio calculations permit also understanding the sizable differences observed in the vibrational spectra. For instance, in the $CO_2-C_6F_6$ dimer, the bending mode of CO_2 is Raman inactive, whereas for $CO_2-C_6H_6$ the corresponding Raman transition is active. We notice that the structure calculated for the complex ab initio is an idealized representation of the complex formation in the dense phase. Indeed, we do not expect that the molecular symmetry axis of the linear molecule remains always perpendicular to the benzene ring due to intermolecular interactions of the heterodimer with its environment. A slight tilt of the molecular axes leads to a removal of the degeneracy of the bending mode of the CO_2 moiety with a subsequent Raman activity. We surmise that this would explain the origin of the weak feature observed in the bending mode domain. However, the experimental difficulty of revealing the corresponding transition suggests that the activity of the mode is very weak. Hence, we can conclude that the local ordering in the mixture should not be very different from that predicted ab initio.

We can understand through the same type of reasoning the polarization and activity of the feature observed between the dyad peaks. Indeed, the correlation between the $D_{\infty h}$ group of the isolated CO_2 molecule and the C_{6v} point group of the heterodimer shows that the Δ_g mode remains degenerated and depolarized (E mode). This prediction is not experimentally supported. In contrast, the point group of the complex in which CO_2 is slightly tilted is C_s and the correlation method applied to this new group shows that the degeneracy of the E mode is removed, leading to the apparition of A′ (polarized) and A″ (depolarized) modes. We therefore conclude that the weak feature observed between the dyad peak is mostly due to the A′ transition and that the A″ activity is negligible compared to the other one. These conclusions are consistent and in agreement with observations reported for CO_2 diluted in other systems as well.[1,3]

Finally, it is appealing to try to interpret the greater solubility of CO_2 in hexafluorobenzene compared to that in benzene on the basis of the complex formation as proposed here. First of all, we may think that the energetic contribution in the formation of the complex may provide a clue to explain the difference between the values of the solubility. Therefore, we would expect that the absolute value of the stabilization energy of the CO_2−hexafluorobenzene heterodimer should be greater than that associated with CO_2−benzene. However, this is not verified as not only the reverse trend is obtained but also the values do not present a sizable difference (−1.88 and −2.38 kcal/mol for CO_2 in C_6F_6 and in C_6H_6, respectively). The energy values are taken here from ab initio calculations limited to a pair of molecules, and it might be argued that realistic calculations should take into account interactions of CO_2 with a number of neighbors. However, even taking into account multibody interactions and their cooperative effects in energy terms, we do not expect that the stabilization energy of CO_2 in C_6F_6 might be so much increased that its value becomes almost twice that of CO_2 in benzene, as is the case for the solubility of CO_2 in the former system for concentrations $x_{CO_2} \leq 0.2$. Thus, the solubility difference cannot be understood by taking only into account energetic considerations.

We can argue that the entropic contributions stemming from the local ordering should play a key role in understanding the difference in the solvating power. The local order existing in C_6H_6 and C_6F_6 pure liquids which is different should not be severely disturbed by adding small amounts of CO_2 (say at pressure ≤1 MPa, Figure 2). Therefore, we may infer that the solubility difference should come from the fact that the local ordering in the pure liquids allows accommodating differently the solute molecules.

At this level of the discussion, it is worthwhile to compare our conclusions about the relative solubility of benzenic compounds in CO_2 with the results obtained in thermodynamics investigations. These works generally deal with the interpretation of the solvation processes in the context of Henry's law, which is valid for very dilute solutions, and therefore we cannot envisage making here a quantitative discussion. However, it has been shown in these investigations that the scaled particle theory (SPT) provides a valuable theoretical framework to capture the

physics of the processes involved in the solvation phenomenon. According to SPT, the solubilization of a solute in a solvent involves two main steps, namely, the creation of a cavity in the solvent of suitable size to accommodate the solute molecule followed by the introduction of the solute into the cavity according to some potential law.[15] In this framework, the Henry constant (hence the solubility) is shown to be related to the sum of the partial molar Gibbs energy of the cavity formation and that associated with the solute−solvent interaction. Such calculations have been performed for gaseous CO_2 (1 atm pressure in the range 10−25 °C) diluted in benzene and hexafluorobenzene.[35−37] It has been found that the value of the calculated solubility in hexafluorobenzene is higher than that in benzene, in agreement with the experimental trend, but that both values underestimate (by about a factor of 2) the experimental ones. This discrepancy has been attributed to the underestimation of the value of calculated molar Gibbs energy of interaction in both solvents, a fact interpreted as due to a complex formation which has not been taken into account in the calculation.[35] Clearly, our study agrees with the point of view of thermodynamics concerning a complex formation of CO_2 with hexafluorobenzene and with benzene. We also note that our ab initio calculations which consider explicitly the formation of a complex agree with the calculations reported before which found that the solute−solvent interaction energy is higher for CO_2−benzene than for CO_2−hexafluorobenzene (implicitly assuming that the Gibbs free energy of interaction can be approximated by the internal energy of interaction as has been done in solubility calculations using SPT).

Interestingly, we also note that the Gibbs energy of cavity formation calculated using SPT represents a significant contribution to the total Gibbs energy of solvation and that the work to make a cavity capable of hosting the CO_2 molecule is greater in benzene than in hexafluorobenzene.[35] This last consideration embodies implicitly the role of the local ordering existing in the two solvents in connection with the solvation process that we have mentioned previously. However, a deeper discussion of the quantitative application of SPT does not appear realistic here as it has been recognized as rather delicate. Indeed, it has been pointed out that the Gibbs energy of cavity formation is strongly sensitive to solvent radii which in turn are not uniquely defined as real molecules are not spheres.[38] For instance, it is easy to show that a 4% correction on the hard sphere diameter of the benzenic solvents is able to exactly reproduce the experimental solubility values. Finally, it comes out that the main issues raised by thermodynamic considerations, namely the free excluded volume and the solute−solvent interactions, are qualitatively supported by the results obtained in our studies.

6. Conclusion

One of the main issues coming from this study is to show that in the CO_2−hexafluorobenzene mixtures, the CO_2 molecules either interact in a nonspecific manner with the surrounding cage molecules or interact specifically with C_6F_6 to form a transient heterodimer. The existence of this transient complex has been evident from the features observed in the forbidden ν_2 bending region, in the spectral domain of the $\nu_1-2\nu_2$ Fermi dyad, and from the strong hindering of the rotational dynamics of carbon dioxide in the mixture. Ab initio calculations have supported the viewpoint of a heterodimer formation and provided the main energetic, structural, and vibrational spectroscopic characteristics of the dimer. The complex is predicted to have an axial structure in which the activity of the ν_2 bending vibration of carbon dioxide is negligible. The experimental difficulty found in the detection of an extremely weak feature in the ν_2 bending mode region suggests that only a modest deviation from the predicted structure should exist in the dense phase. Finally, the present study reinforces the conclusions of our previous studies concerning the vibrational spectroscopic domain of interest and their analysis to put in evidence the formation of transient heterodimers in CO_2−organic solvent mixtures. Moreover, we emphasize again the importance of ab initio calculations in interpreting dense phase experiments. We conclude in agreement with our previous studies that ab initio calculations are predictive because the elementary act of formation of the transient complex involves a time scale which matches the observation time of Raman spectroscopy.

Acknowledgment. The University of Bordeaux 1 and the Fundação para a Ciência e Tecnologia (Portugal) are acknowledged for the financial support of M.I.C. The joint CNRS−GRICES PIC Program No. 3090 has provided travel and temporary residence facilities for M.I.C. and M.B. to complete part of this work. The authors are pleased to thank David Talaga and Jean-Luc Bruneel of the ISM for valuable help in Raman measurements. Finally, the authors gratefully acknowledge the support provided by the IDRIS computer center of the CNRS (Institut du Développement et des Ressources en Informatique Scientifique, Orsay) for allocating computing time and providing facilities.

References and Notes

(1) Besnard, M.; Cabaço, M. I.; Longelin, S.; Tassaing, T.; Danten, Y. *J. Phys. Chem. A* **2007**, *111*, 13371–13379.
(2) Cabaço, M. I.; Danten, Y.; Tassaing, T.; Longelin, S.; Besnard, M. *Chem. Phys. Lett.* **2005**, *413*, 258–262.
(3) Besnard, M.; Cabaço, M. I.; Talaga, D.; Danten, Y. Submitted for publication, 2008.
(4) Cabaço, M. I.; Danten, Y.; Besnard, M.; Guissani, Y.; Guillot, B. *J. Phys. Chem. B* **1997**, *101*, 6977–6987.
(5) Danten, Y.; Cabaço, M. I.; Tassaing, T.; Besnard, M. *J. Chem. Phys.* **2001**, *115*, 4239–4248.
(6) Tassaing, T.; Cabaço, M. I.; Danten, Y.; Besnard, M. *J. Chem. Phys.* **2000**, *113*, 3757–3765.
(7) Shen, J. W.; Domanski, K. B.; Kitao, O.; Nakanishi, K. *Fluid Phase Equilib.* **1995**, *104*, 375–390.
(8) McHugh, M. A. In *Encyclopedia of Polymer Science and Engineering*; John Wiley & Sons, Inc.: New York, 1989.
(9) Kazarian, S. G.; Vincent, M. F.; Bright, F. V.; Liotta, C. L.; Eckert, C. A. *J. Am. Chem. Soc.* **1996**, *118*, 1729–1736.
(10) Meloa, M. J. P.; Dias, A. M. A.; Blesic, M.; Rebelo, L. P. N.; Vega, L. F.; Coutinho, J. A. P.; Marrucho, I. M. *Fluid Phase Equilib.* **2006**, *242*, 210–219.
(11) Kazarian, S. G.; Gupta, R. B.; Clarke, M. J.; Johnston, K. P.; Poliakoff, M. *J. Am. Chem. Soc.* **1993**, *115*, 11099–11109.
(12) Costa-Gomes, M. F.; Padua, A. A. H. *J. Phys. Chem. B* **2003**, *107*, 14020.
(13) McHugh, M. Thermodynamics 2007, Rueil-Malmaison, France, 2007.
(14) Reiss, H.; Frish, H. L.; Helfand, E.; Lebowitz, J. L. *J. Chem. Phys.* **1960**, *32*, 119.
(15) Pierotti, R. A. *Chem. Rev.* **1976**, *76*, 717.
(16) Frisch, M. J.; et al. *Gaussian 03*; Gaussian Inc.: Wallingford, CT, 2004.
(17) Møller, C.; Plesset, M. S. *Phys. Rev.* **1934**, *46*, 618.
(18) Dunning, T. H. *J. Chem. Phys.* **1989**, *90*, 551.
(19) Wilson, A. K.; Mourik, T. V.; Dunning, T. H. *J. Mol. Struct.* **1996**, *388*, 339.
(20) Tatewaki, H.; Huzinaga, S. *J. Comput. Chem.* **1980**, *3*, 205.
(21) Kendall, R. A.; Dunning, T. H.; Harrison, R. J. *J. Chem. Phys.* **1992**, *96*, 6796.
(22) Boys, S. F.; Bernardi, F. *Mol. Phys.* **1970**, *19*, 553.
(23) Wilson, E. B.; Decius, J. C.; Cross, P. C. In *Molecular Vibrations*; McGraw-Hill: New York, 1955.
(24) Cabaço, M. I.; Longelin, S.; Danten, Y.; Besnard, M. *J. Chem. Phys.* **2007**, *128*, 74507.
(25) Scott, A. P.; Radom, L. *J. Phys. Chem.* **1996**, *100*, 16502–16513.
(26) Gupta, M. K.; Li, Y.-H.; Hulsey, B. J.; Robinson, R. L., Jr. *J. Chem. Eng. Data* **1982**, *27*, 55.

(27) Chrastil, J. *J. Phys. Chem.* **1982**, *86*, 3016.
(28) Nakayama, H.; Murai, M.; Tono-oka, M.; Masuda, K.; Ishii, K. *J. Phys. Chem. A* **2007**, *111*, 1410–1418.
(29) Lalanne, P.; Rey, S.; Cansell, F.; Tassaing, T.; Besnard, M. *J. Supercrit. Fluids* **2001**, *19*, 199–207.
(30) Cabaço, M. I.; Longelin, S.; Danten, Y.; Besnard, M. *J. Phys. Chem. A* **2007**, *111*, 12966–12971.
(31) Garrabos, Y.; Tufeu, R.; Neindre, B. L.; Zalczer, G.; Beysens, D. *J. Chem. Phys.* **1980**, *72*, 4637–4661.
(32) Adams, J. E.; Siavosh-Hagahighi, A. *J.Phys. Chem. B* **2002**, *106*, 7973–7980.
(33) Versmold, H. *Mol. Phys.* **1981**, *43*, 383.
(34) Cabaço, M. I.; Besnard, M.; Tassaing, T.; Danten, Y. *J. Mol. Liq.* **2006**, *125*, 100–106.
(35) Wilhelm, E.; Battino, R. *J. Chem. Thermodyn.* **1971**, *3*, 761–768.
(36) Wilhelm, E.; Battino, R. *J. Chem. Thermodyn.* **1971**, *3*, 753–760.
(37) Wilhelm, E.; Battino, R. *J. Chem. Thermodyn.* **1971**, *3*, 409.
(38) Tang, K. E. S.; Bloomfeld, V. A. *Biophys. J.* **2000**, *79*, 2222−2234.

JP8068267